ANNUAL REVIEWS

*Annual Review of Earth and Planetary Sciences*

# Earthquake Early Warning: Advances, Scientific Challenges, and Societal Needs

Richard M. Allen[1] and Diego Melgar[2]

[1]Department of Earth and Planetary Science, University of California, Berkeley, California 94720-4760, USA; email: rallen@berkeley.edu

[2]Department of Earth Sciences, University of Oregon, Eugene, Oregon 97403-1272, USA; email: dmelgarm@uoregon.edu

Annu. Rev. Earth Planet. Sci. 2019. 47:361–88

First published as a Review in Advance on January 30, 2019

The *Annual Review of Earth and Planetary Sciences* is online at earth.annualreviews.org

https://doi.org/10.1146/annurev-earth-053018-060457



## Keywords

earthquake early warning, hazard reduction, earthquake physics, ground motion prediction, seismic networks, geodetic networks

## Abstract

Earthquake early warning (EEW) is the delivery of ground shaking alerts or warnings. It is distinguished from earthquake prediction in that the earthquake has nucleated to provide detectable ground motion when an EEW is issued. Here we review progress in the field in the last 10 years. We begin with EEW users, synthesizing what we now know about who uses EEW and what information they need and can digest. We summarize the approaches to EEW and gather information about currently existing EEW systems implemented in various countries while providing the context and stimulus for their creation and development. We survey important advances in methods, instrumentation, and algorithms that improve the quality and timeliness of EEW alerts. We also discuss the development of new, potentially transformative ideas and methodologies that could change how we provide alerts in the future.

- Earthquake early warning (EEW) is the rapid detection and characterization of earthquakes and delivery of an alert so that protective actions can be taken.
- EEW systems now provide public alerts in Mexico, Japan, South Korea, and Taiwan and alerts to select user groups in India, Turkey, Romania, and the United States.

- EEW methodologies fall into three categories, point source, finite fault, and ground motion models, and we review the advantages of each of these approaches.
- The wealth of information about EEW uses and user needs must be employed to focus future developments and improvements in EEW systems.

## 1. INTRODUCTION

Earthquake early warning (EEW) is the delivery of ground shaking alerts or warnings. It is distinguished from prediction in that the earthquake has nucleated to provide detectable ground motion when an EEW is issued. The warning time available is the time between detection and when ground motion is experienced by a user. Potential warning times are therefore seconds to minutes. Likewise, the time available to collect and process geophysical data and deliver alerts is seconds to minutes, and the actions of users must be possible in seconds to minutes.

The concept of EEW has been around for as long as there have been electronic communications that can outpace seismic waves. Following the 1868 earthquake on the Hayward Fault, J.D. Cooper (1868) proposed that the new telegraph cables that radiated away from San Francisco could be used to transmit a warning to the city and a characteristic bell would ring the alarm. While the concept is simple, the implementation is much more complex. How do you detect an earthquake? How do you determine the size (magnitude or otherwise) of the event and the distance to which ground shaking will be felt or damaging? How quickly can you do this, and how accurately? How do you choose the right trade-off between speed and accuracy? Who should receive alerts? How should the alerts be communicated (both message content and delivery technology) to different classes of users? How accurate do the alerts need to be? Since no system can be perfect, what is the tolerance for false and missed alerts? Who should pay for the system (government versus private sector/users)? Who is responsible for its successes and failures?

While EEW has its foundation in earthquake science, and it is earthquake scientists who have predominantly developed the concept and been responsible for the implementation, the success of an early warning system is dependent on many stakeholders working together to bring an EEW system into operation in each region. For example, ShakeAlert is the US EEW system that is currently being tested with pilot users in California, Oregon, and Washington. The phased rollout of alerts to the entire population is now underway because the network infrastructure is complete. Key individuals who are making this possible include (*a*) political leaders at the city, state, and federal levels; (*b*) leadership at state and federal agencies responsible for risk reduction and disaster mitigation; (*c*) leadership in the private sector representing EEW business applications; and (*d*) the earthquake science community spanning geophysics, social science, and disaster mitigation. It is important to recognize that without this broad collaboration, communication, and engagement, EEW will achieve little.

**ShakeAlert:** earthquake early warning system in the United States currently generating alerts in California, Oregon, and Washington

So, what are the key components of a successful EEW system? The most important component is a group of users who want alerts and can define the necessary capabilities of the system. As described in the next section, the gradual development of EEW around the world over the last few decades provides a great deal of information about who the potential users are and what they want and need. Next is the physical infrastructure for a system. Two physical networks are needed, one that provides the data to detect and characterize earthquakes and a second that can deliver the alerts. These networks include sensors, communications and telemetry, processing capabilities, and receivers to deliver the alerts. With the growth of the Internet of Things, these could be the

same network. Finally, intellectual community and capacity are needed to distill the sensor data into alerts and deliver them in a useful and usable format to users. This is, of course, a collaborative effort between physical and social earthquake scientists.

There is also one additional characteristic of EEW that perhaps makes it unique in earthquake science. An operational EEW system makes testable predictions about the earthquake process and physics every day. Every time an EEW system detects or alerts on an earthquake, we test the earthquake model used by the underlying EEW algorithms. Even more unique is the fact that members of the public are able to evaluate the success or failure of our daily predictions when they do, or do not, receive an alert for a felt earthquake. This is very different from other products the earthquake science community provides. For example, earthquake forecasts of all types (e.g., hazard maps) provide a probability that there will be an earthquake, and correspondingly there is a probability that there will not be a large earthquake. Whether an earthquake occurs or not, the forecast is correct, which makes it untestable or at least difficult to understand and interpret from the public perspective. This is perhaps at the heart of why EEW is so important in our efforts to reduce earthquake risk: It is actionable information for every member of the public, and the public can and will immediately assess if our information was correct or not. This provides a challenge and an opportunity. This is why it is so important that we, the earthquake science community, get it right.

In this review we aim to gather information about existing EEW systems around the world and the ongoing development of methods and algorithms to improve the quality and timeliness of EEW alerts. We start with a review of EEW users based on various studies around the world. We then review the status of EEW systems implemented in various countries, providing the context and stimulus for their creation and development. Next we review the development of new ideas and methodologies for EEW algorithms. Finally, we review some new concepts for EEW that could change how we provide alerts in the future.

## 1.1. Framing the Problem: User Needs

There are three broad categories of EEW users: (*a*) individuals receiving alerts who make personal decisions about how to respond, (*b*) automated response applications that typically require institutions or companies to make decisions about how to apply and implement automated alert responses, and (*c*) individuals and institutions who want rapid earthquake information for situational awareness purposes. It is also important to consider which users are more or less likely to use a warning system. Who are the early adopters, and for whom does EEW adoption represent a significant expense and/or effort?

Perhaps the most important category of users is the public, broadly defined as a group of individuals who want personal alerts and will take personal protective actions. The impact of public alerts and responses is perhaps the clearest case of the cost-benefit of EEW. In the 1989 Loma Prieta earthquake in the San Francisco Bay Area, more than 50% of injuries were linked to falls; in the 1994 Northridge earthquake in Southern California, more than 50% of injuries were due to nonstructural falling hazards (i.e., things falling on people rather than building collapse) (Shoaf et al. 1998). This means that if everyone got a few seconds' warning of coming shaking and dropped, took cover, and held on, the number of injuries in an earthquake could be halved (Strauss & Allen 2016). The estimated cost of injuries alone in the moderate M6.7 1994 Northridge earthquake was $2–3 billion (Porter et al. 2006).

Many members of the public also fall into the category of early adopters in that they are keen to receive the alerts as soon as possible. EEW is very popular with the public even in the face of limited or even poor performance. A survey of the public in Japan one year after the M9.1 Tohoku-Oki

earthquake on March 11, 2011, asked the question, "Is EEW useful?" (Hoshiba 2014). Nationally, 82% of those surveyed responded positively, and in the Tohoku-Oki region, 90% responded positively. This was despite the fact that the warning for the M9.1 event was issued only in the epicentral region and there were many alerts during the intense aftershock phase for which people did not feel shaking due to incorrect associations and poor event locations (Hoshiba 2014). In a less-formal survey of EEW users in Mexico City following events in September 2017, users had a similarly positive response despite the fact that the alert was issued after most people felt shaking in the most-damaging M7.1 September 19, 2017, Puebla event, and there had been several other alerts in the same month for events in which most people did not feel shaking (Allen et al. 2017, 2018). In California, where there is currently no fully public warning system, a poll by Probolsky Research in 2016 found that 88% of the sampled population supported building a statewide EEW system, and 75% were willing to pay an additional tax to fund it. This is encouraging for EEW developers: The public wants alerts and is accepting of imperfect warning systems.

**Modified Mercalli Intensity (MMI):** scale used to describe the shaking intensity at a given location; varies with distance from the epicenter of an earthquake

So what type of alerts does the public want and need? We know that effective alerts must be simple while delivering information about both the hazards and the actions to be taken (Wood et al. 2012). While individuals may be in many different types of hazardous situations during an earthquake, the default response message for EEW must be simple, just as it is for the response if you feel shaking: "Drop, cover, and hold on." What is notable is that providing information about shaking intensity or time to shaking is neither needed nor desirable. Most people do not understand the difference between intensity and magnitude, so including it causes confusion. Providing a countdown can also delay response as a user digests the additional information and contemplates action. In Mexico City a simple siren sounds across the city (Cuéllar et al. 2014). In Japan the broadcast alert is also simple: "Earthquake Early Warning. An earthquake has occurred in Area X. Please prepare for a strong temblor" (Seki et al. 2008, p. 3).

The next question is, which area to alert? As the message contains an action to be taken, the goal is to deliver that alert only to the people who should drop, cover, and hold on—that is, the users who are likely to be impacted by the earthquake. Ground motion is inherently a stochastic process. There will always be variability in the intensity of shaking from one location to the next that can only be described statistically (e.g., Atik et al. 2010). This variability is typically a factor of two, which corresponds to approximately one intensity level. If the goal is to alert all people who might feel shaking, we must choose whether to alert areas where the predicted Modified Mercalli Intensity (MMI) is II, meaning some people indoors feel the shaking, or IV, when many feel shaking outside. When making this choice, we must consider the relative tolerance of the public user for what is perceived as an unnecessary alert versus no alert when the user expected one. More work is needed in this area, as there is little quantitative information as to the tolerance of different users to false and missed alerts. However, some guidance may come from user perceptions in Mexico City. When people were asked what they considered to be a false alert, their general response was an alert when there was no earthquake (Allen et al. 2017, 2018). It was not an alert with no felt shaking. This implies that users are more tolerant of unnecessary alerts than of missed alerts.

A subset of this public group of alert users includes individuals who work in situations that are more hazardous than typical offices. Examples include construction workers on building sites, utility workers who might be climbing high-voltage power lines, and people working with hazardous chemicals or heavy machinery. While the hazard is related to the work environment and the responsibility for providing a safe work environment may lie with the employer, it is still the human responses of the individuals that are the most effective mitigation: stepping away from hazards, stopping machinery, putting down chemicals, securing safety harnesses, and so on. In a survey of potential industrial users for ShakeAlert in California, these human-response actions

were unanimously identified as being of the greatest value (Johnson et al. 2016). These individual users have the same need of a simple warning but require more specialized education and training on how to respond to the alerts.

The public is also a good early adopter group because the daily life or work impact of adopting EEW is minimal and has broader positive benefits. If the actions to be taken are simply to drop, cover, and hold on, or to step away from hazards at the workplace, then the cost of these actions is minimal—just a few minutes. When this is done in a damaging earthquake, the actions can significantly reduce injuries, fatalities, and costs. Also, training people to take these actions and having people respond to an earthquake alert even when the shaking is not that severe for them have the benefit of building a seismic culture of preparedness and thereby increasing the resiliency of a community. This encourages people to think about earthquakes, the impacts, and their responses and preparedness (Allen et al. 2017, 2018).

The second category of users is automated response applications. The list of potential applications is long and includes slowing and stopping trains, preventing planes from taxiing and landing, taking elevators to the ground floor and opening doors, automatically isolating hazardous chemicals, and stopping heavy and hazardous machinery. The examples of where these applications have been implemented are more limited.

By far the most commonly implemented automated response application is slowing and stopping trains. EEW has been part of the Japanese Shinkansen system since the 1960s and automatically slows and stops trains when earthquakes are detected (Nakamura & Tucker 1988). The high-speed trains in China are now also spurring the development of EEW systems. In the San Francisco Bay Area, the Bay Area Rapid Transit (BART) train system was a very early adopter and integrated EEW alerts into the train control system in 2012 when ShakeAlert was still a research project (Strauss & Allen 2016). Two aspects of this application make train systems early adopters: (*a*) the very serious potential consequences of earthquake shaking and (*b*) the ease of implementation coupled with the low costs and consequences of taking action. A potential consequence of earthquake shaking is train derailment, which is more likely if a train is traveling at high speed and can result in many injuries and casualties. The ease of implementation is related to the automated nature of train control. BART automatically accelerates and decelerates trains in and out of stations. The same automated train control systems that make it easy to implement EEW also mean that the cost of slowing and stopping a train when the shaking is not that severe is low. Trains can be restarted as soon as the operators are ready, minimizing the impact on riders. Elevators are another example. It is easy to have them go to the ground floor and open the doors, preventing hundreds of people from being trapped.

The inverse of the above examples also appears to be true. EEW applications with significant costs of implementation and/or significant costs or consequences of taking alert actions are unlikely to be implemented. This is true irrespective of how high the consequences of earthquake shaking are. Nuclear power plants are unlikely to use EEW (Cauzzi et al. 2016), as the cost of implementing an emergency shutdown is significant because it shortens the lifetime of the reactor.

The third category of users is situational awareness users. This refers to operational centers who want and need to be aware of events that threaten infrastructure. This includes emergency operations centers such as 911 centers and telecommunication, power, and other utility operations. Having this information available allows them to understand possible causes of system disruption and also reduce the impact by preventing cascading hazards. This group is also a very early adopter of EEW, as having any additional source of information automatically streaming into these centers is valuable.

The purpose of this summary is to draw conclusions about the types of information EEW users want and need. First, for all the applications described, once an alert is issued, the response will

likely be completed and the users will then wait for a period of minutes before resuming normal activities. People will drop, cover, and hold on, and then they will wait for the shaking to stop or wait to be sure that they will not feel shaking. Trains or elevators will stop, and operators will wait to be sure the hazard has passed before restarting. In this sense, the alert cannot be taken back; instead, once the alert is triggered, people will wait for an all clear. Second, because of all the complexity and uncertainty when an earthquake is underway, the information must be reduced to a very simple form for the alert decision to be made. All examples of known users are looking for a binary alert: react when an alert is issued; otherwise no alert should be issued. As most users will want to react when shaking is expected to be above some threshold, the information about the earthquake must be reduced into a map of shaking intensity and then an alert issued to the appropriate region for different categories of users. It is not the case that detailed earthquake information (locations and magnitudes) can be sent to all users who will then decide whether to react.

**Ground motion prediction equation (GMPE):** estimates the distribution of ground shaking for an earthquake based on distance from the fault, local site conditions, and other parameters

## 1.2. Approaches to Alert Generation

Now that we know who the users are and what they need, we can next consider the nature of the alerts that are possible given the constraints of earthquake physics. **Table 1** provides a summary of the relevant distances and timescales for EEW for various magnitude earthquakes. We use MMI V as the threshold when EEW is most useful. MMI V is described as "felt by nearly everyone; many awakened. Some dishes, windows broken. Unstable objects overturned." It is the lower threshold for when we expect to see some light damage. One could argue that EEW is useful over a much wider area—anywhere an earthquake is felt (i.e., MMI $\geq$ II), as even people in a region where shaking is felt but is unlikely to cause damage can benefit from knowing that while they are about to feel shaking, the hazard is minimal. Also, such alerts serve as an EEW drill and help build a culture of seismic prevention (Allen et al. 2018).

The S-wave arrival time at the greatest distance where MMI V is expected and the approximate end of peak shaking are included to give a sense of the total time available to provide an alert and act in response to it. These numbers are only an approximate guide for several reasons. The shaking intensity at any specific location can vary by a factor of two (Worden et al. 2010) compared to the average shaking at that distance according to ground motion prediction equations (GMPEs). Also, the strongest shaking can be significantly later than the S-wave arrival time. A compilation of peak shaking observations for large-magnitude events ($M > 6$) shows that peak shaking occurs up to 10 s after the S-wave at 50 km and up to 50 s at 400 km (Allen 2011).

**Table 1 Approximate estimates of relevant distances and times for earthquake early warning applications**

| Magnitude | Approximate fault length | Approximate distance from fault where MMI $\geq$ V | Maximum epicentral distance where MMI V is expected | S-wave arrival time at maximum distance where MMI V is expected | Approximate end of peak shaking |
|---|---|---|---|---|---|
| M5 | 1 km | 8 km | 10 km | 4 s | 10 s |
| M6 | 6 km | 30 km | 40 km | 10 s | 20 s |
| M7 | 50 km | 100 km | 200 km | 40 s | 60 s |
| M8 (crustal) | 400 km | 300 km | 700 km | 200 s | 300 s |
| M9 (subduction) | 1,000 km | 400 km | 1,000 km | 300 s | 600 s |

All numbers are one significant figure and are intended to give outer bounds to the time-space region where MMI $\geq$ V may occur. Abbreviation: MMI, Modified Mercalli Intensity.

While the area that can be affected by a large-magnitude earthquake can be huge, most of the damage caused by earthquakes will almost always be at smaller epicentral distances and close to the rupturing fault. Therefore, providing an initial alert within a few seconds (**Table 1**) is the most critical objective for any EEW system so that alerts can be provided as close as possible to the epicenter. Following this initial alert, there is time to provide better information or alert a larger region in the tens of seconds that follow for larger events ($M > 7$) (**Table 1**).

For this reason, all regional EEW systems use a point source algorithm. These typically use a few seconds of P-wave data (0.5–4 s) from a handful of stations (two to six) close to the epicenter to detect an earthquake and characterize location, origin time, and magnitude (Allen & Kanamori 2003). This information can be transformed into ground shaking information for users employing an appropriate GMPE. These algorithms have the advantage of being fast; they usually provide the earliest warning and therefore the most warning time. However, their predictions typically saturate for ~M7 earthquakes (**Figure 1**) for two reasons. First, it is difficult or impossible to distinguish an M8 earthquake from an M7 when only information about the first few seconds of the source time function (STF) is known. Second, for ruptures extending hundreds of kilometers along a fault, the shaking intensity that a user should expect is dependent on the magnitude and distance to the fault rupture, and the lateral extent of the rupture is not provided by point source information.

Finite fault algorithms aim to remedy the point source saturation issue by estimating the finite extent of the rupture. They also typically improve the magnitude estimate by reducing or removing the magnitude saturation limitation (Colombelli et al. 2013). Both seismic and geodetic approaches are being used to accomplish these goals. While finite fault algorithms are slower than point source algorithms, they can predict higher intensities of shaking, and over larger areas, for the largest earthquakes before the shaking is felt (Ruhl et al. 2019a) (**Figure 1**).

The last category of algorithms includes ground motion models (GMMs). These are very different in that they do not attempt to characterize the earthquake source at all. Instead, they use observations of strong shaking to forward predict shaking at other locations (Hoshiba & Aoki 2015). Their advantage is that they are not susceptible to the challenges of earthquake detection, association of seismic arrivals from multiple stations, uncertainties in location, and uncertainties

**Source time function (STF):** seismic moment release as a function of time for a given earthquake

**Ground motion model (GMM):** approach to earthquake early warning where observations of ground motion are directly used to estimate future ground motion

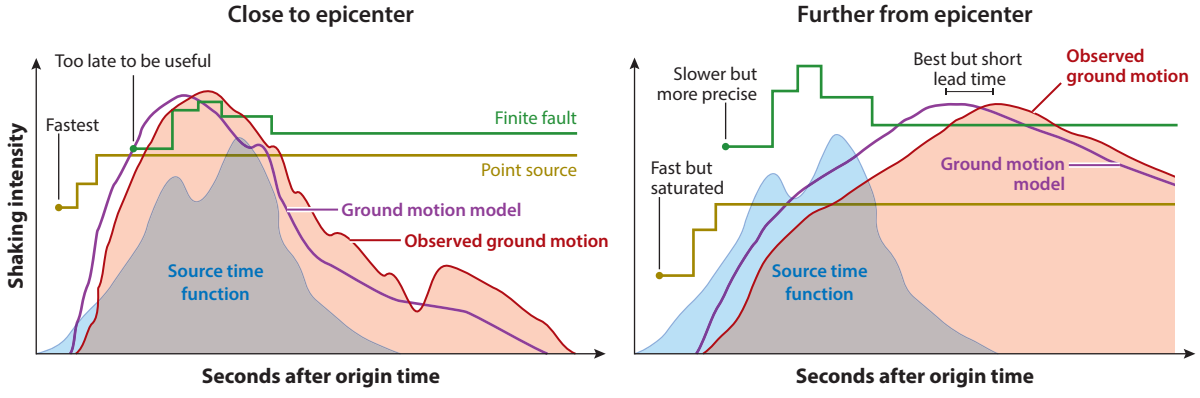


**Figure 1**

Conceptual sketch of expected earthquake early warning shaking forecasts during a moderate to large event (*left*) close to the epicenter and (*right*) further away. The earthquake source time function (*blue region*) indicates the duration and character of rupture. Also shown are the actual ground motion expected at each location (*pink region*) and the intensity forecasts for a point source algorithm (*gold line*), a finite fault algorithm (*green line*), and a ground motion model (*purple line*).

in magnitude. This can be particularly difficult during aftershock sequences, during earthquake swarms, or for the largest magnitude events (M9). The disadvantage is that the accuracy of the ground shaking prediction decreases as a function of the warning time. Forward predictions of more than ~10 s are perhaps too uncertain to be useful (**Figure 1**).

**SASMEX:** earthquake early warning system in Mexico that broadcasts alerts including to a loudspeaker system that can be heard across Mexico City

One last approach is the onsite method that uses data from a sensor at a site to detect an earthquake and generate an alert at the same site. The most basic version of this method is a simple ground motion threshold that sounds an alert at the same time the detected shaking is unusual or reaches a damaging level. More sophisticated systems detect P-waves and trigger an alert when the following S-wave or peak shaking is predicted to be large.

## 2. EARTHQUAKE EARLY WARNING IMPLEMENTATION AROUND THE WORLD

The implementation of EEW has been driven by the advent of digital seismic instrumentation and digital communications to collect the data and issue alerts. The availability of these technologies has spurred the expansion of seismic networks, and the resulting data have then improved our physical earthquake models to provide a framework for generating alerts.

But the development of EEW has also been driven by several key earthquakes. The 1985 M8.1 Mexico City earthquake killed more than 20,000 people in the city and illustrated that there could be more than 1 min between when seismic stations detected the event along the coast and when the shaking was felt in Mexico City. Mexico City's EEW system became operational in 1991. The 1995 M6.9 Kobe earthquake killed more than 6,000 people and led to the deployment of multiple dense seismic networks across Japan that were then used to develop an early warning capability that became public in 2007. The 2008 M7.9 Wenchuan earthquake in China killed 70,000 and initiated the development of EEW in the region. One of the greatest tests of EEW systems was the 2011 M9.1 Tohoku-Oki earthquake. While an alert was successfully issued, this event and its aftershocks highlighted potential areas for methodological improvements (see Section 3). This event in Japan also placed the EEW research effort in the United States on a path toward public implementation. Finally, the 2018 M7.1 Puebla earthquake in central Mexico was the most significant test of the Mexican EEW system and provided insights into the public response and attitude toward EEW.

Here we summarize the current operational characteristics of EEW systems around the world. We divide the systems into three categories (**Figure 2**; **Table 2**). Japan and Mexico have public alert distribution where the alerts are broadcast through multiple channels and are available to all members of the public. South Korea and Taiwan also provide public alerts to cell phones and smartphones. Several regions have limited alert distribution where alerts are distributed to some groups of users. These often include train operators, schools, and emergency service groups. Finally, system construction is underway in many more regions where real-time testing and development are in progress, but these alerts are not yet being issued to users beyond the earthquake science and engineering community.

Allen et al. (2009) reviewed the history and status of EEW systems around the globe at that time, so here we focus on the changes, improvements, and expansions over the last decade. Clinton et al. (2016) also reviewed efforts in Europe.

Mexico's SASMEX system operated by CIRES (Espinosa-Aranda et al. 1995) has expanded significantly and now covers multiple states and cities. Alerts are issued through thousands of dedicated radio receivers deployed in schools and government offices. In Mexico City a public alert sounds 12,000 sirens across the city that can be heard by most residents (Cuéllar et al. 2014). The system still uses the concept of assessing the likely magnitude of a detected earthquake at individual stations. When two stations have detected a significant earthquake, the alert is triggered

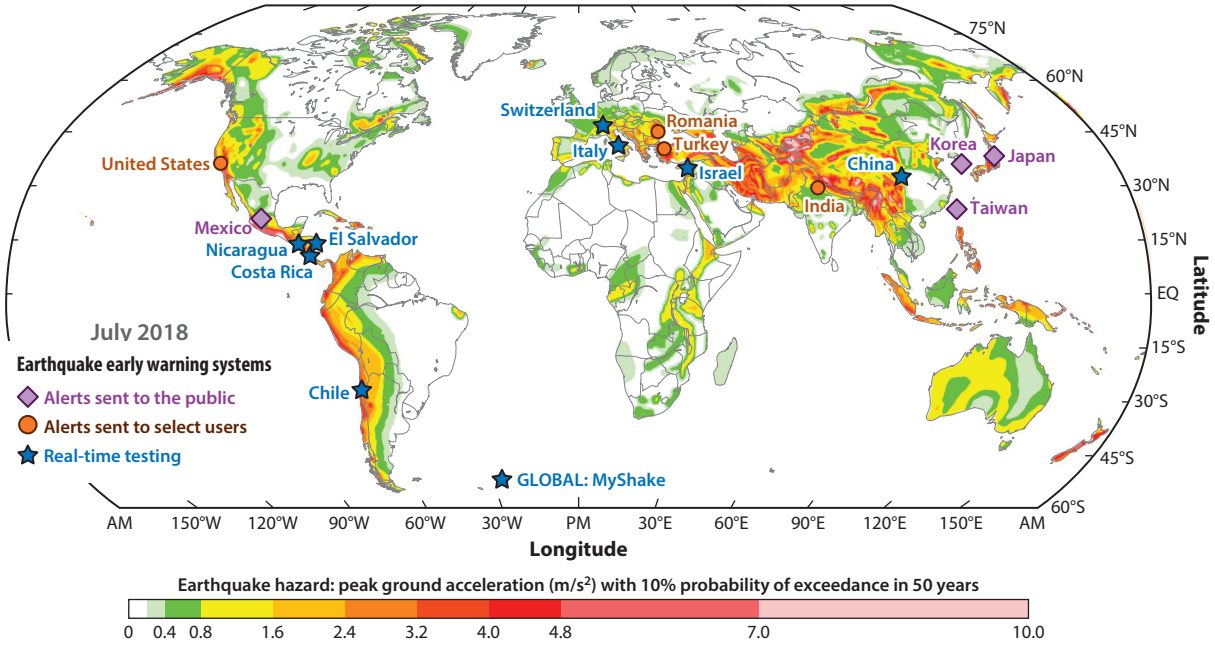


**Figure 2**

Status of earthquake early warning systems in different regions of the globe. Shown are locations of systems that broadcast alerts to all members of the public (*purple*), systems distributing alerts to select users (*orange*), and systems undergoing real-time development and testing (*blue*). The background is the seismic hazard presented as peak ground acceleration with 10% probability of exceedance in 50 years.

in cities likely to experience shaking. The threshold for issuing alerts in Mexico City, for example, is the detection of $M > 5$ earthquakes at two stations as far away as the coast 300 km to the south. The algorithm applied at each site has been improved to require less data to issue alerts faster, now just 3 s of the P-wave (Cuéllar et al. 2018). The system issued alerts for the damaging earthquakes occurring in September 2017, and despite some performance challenges, it is clear that the public perception of SASMEX is very positive (Allen et al. 2017, 2018). It is notable that there are also two independent private-sector EEW systems that are operational, SkyAlert and Grillo. Both run

**Table 2 Status of earthquake early warning systems in different regions of the globe**

| Public alert distribution | Limited alert distribution | System construction |
|---|---|---|
| Alerts broadcast to all members of the public | Alerts distributed to selected users | Real-time testing and development of alert system |
| Mexico: multiple states<br>Japan: nationwide<br>South Korea: nationwide<br>Taiwan: nationwide | India: Roorkee region<br>Romania: regional<br>Turkey: Istanbul<br>United States: West Coast | Chile: nationwide<br>China: several regions<br>Costa Rica: regional<br>El Salvador: regional<br>Israel: nationwide<br>Italy: Irpinia region<br>Nicaragua: regional<br>Switzerland: nationwide<br>Global: MyShake smartphones |

their own detection networks and broadcast the alerts primarily through smartphone apps and to dedicated Internet-connected devices.

**ElarmS:** earthquake early warning algorithm using a few seconds of P-wave data to detect, locate, and estimate the magnitude of an earthquake underway

**Microelectro-mechanical system (MEMS):** a very compact type of accelerometer such as those found in smartphones and other devices

**Finite fault detector (FinDer):** earthquake early warning algorithm matching observed patterns of ground shaking with templates to estimate future shaking

The 2011 M9.1 Tohoku-Oki earthquake was a substantial test for Japan's public alert system operated by the Japan Meteorological Agency (JMA) (Hoshiba 2014). In 2011, a point source algorithm was being used to locate earthquakes based on P-wave arrival times and estimate the magnitude from the first few seconds of the P-wave. An alert was issued across the most severely affected Sendai region, where the expected ground shaking exceeded the public alert threshold of JMA intensity 5-lower (equivalent to MMI VII). However, this massive earthquake caused significant shaking over a much larger area than predicted by the EEW algorithm, as the magnitude estimate saturated at M8.1, and there was no information about the finite extent of the rupturing fault plane, which extended 400 km to the south and caused strong shaking in Tokyo's Kanto region as well. Also, in the intense aftershock sequence, the algorithm incorrectly associated seismic arrivals from separate simultaneous events, resulting in poor-quality alerts for a period of weeks (Hoshiba 2014). JMA has significantly improved the algorithms used since (Kodera et al. 2018), as we discuss in Section 3. The public perception of the JMA system is very positive, and alerts continue to be broadcast through multiple channels (Hoshiba 2014). These include broadcast messages that trigger alerts on most cell phones (Seki et al. 2008); publicly available commercial smartphone apps (e.g., Yurekuru); and TV, radio, and various other dedicated communication channels.

South Korea has been experimenting with EEW for about a decade. The effort started with the evaluation of the ElarmS point source algorithm (Kuyuk et al. 2014, Sheen et al. 2017), which the Korean Meteorological Administration now uses to issue public alerts. Alerts are distributed using the Cell Broadcast System, which can deliver text message–like alerts to all phones simultaneously across the country for $M > 4$ earthquakes. Current efforts are underway to provide more localized and user-specific alerts that include information of what actions to take.

Taiwan is now using a total of three EEW systems. The Central Weather Bureau is the official source of EEW and uses the national seismic network to detect events and issue warnings using a P-wave-based point source approach (Wu et al. 2014). It typically takes 15 s to generate the alert, meaning warnings can be issued to cities more than 50 km from the epicenter, and the alerts are available on all mobile phones. The P-alert system developed by National Taiwan University uses a low-cost microelectromechanical system (MEMS) sensor to provide onsite warnings more rapidly to locations close to the epicenter. It uses P-wave displacement thresholds to issue alerts within the ~600 buildings—most of them schools—that now have P-alert devices installed (Wu et al. 2018). Finally, the National Center for Research on Earthquake Engineering has also developed an onsite approach. It also uses a few seconds of P-wave data to predict the coming peak shaking, but it uses six extracted features and a support vector machine model to decide when to alert. Its devices are currently installed in ~30 locations, primarily schools, and it has plans to expand rapidly (Hsu et al. 2018).

The phased rollout of a public EEW system for the West Coast of the United States (California, Oregon, and Washington) is currently underway. The system is called ShakeAlert and is operated by the US Geological Survey in collaboration with the University of California, Berkeley; the California Institute of Technology; the University of Oregon; the University of Washington; and state emergency management agencies (Kohler et al. 2017). Expansion of the seismic networks will double the number of sensors contributing data to 1,500 over the next few years (Given et al. 2014). The system received extensive testing of multiple approaches (Cochran et al. 2017) and uses a single point source algorithm called EPIC that is primarily based on ElarmS-3 (Chung et al. 2019) and the finite fault detector (FinDer) source algorithm (Böse et al. 2017). Testing is also underway of multiple algorithms that use geodetic data to both improve the magnitude and estimate the finite extent of large ruptures. The phased public rollout in 2018 included stopping

trains, alerts in some schools, and automated water supply management. At the beginning of 2019, the city of Los Angeles made the ShakeAlertLA app available to the public with the intent of delivering alerts in Los Angeles County.

In northern India a network of 84 accelerometers has been deployed by IIT Roorkee around the main central thrust just north of Roorkee. The system takes a point source approach, using peak displacement from 3 s of P-wave data to estimate the magnitude. When an event M6 or greater is detected, an alert is issued that sounds sirens in student dormitories and in emergency control rooms for all districts across Uttarakhand (Chamoli et al. 2019).

In Romania the National Institute for Earth Physics has been providing warnings in the Vrancea region, where very deep earthquakes occur and have damaged Bucharest in the past. Alerts go to a nuclear research facility and the Basarab Bridge, where traffic is stopped. It is using the PRESTo algorithm (Satriano et al. 2010) in addition to its own event validation approach (Mărmureanu et al. 2010), and alerts are now being made more widely available by private companies delivering alerts from the national system (Clinton et al. 2016).

In Turkey Istanbul has a warning system based on a simple exceedance of acceleration threshold at three stations in the network of sensors across the city. The system is operated by the Kandilli Observatory and the Earthquake Research Institute and provides alerts to the Istanbul Gas Distribution Company and the Marmaray Tube Tunnel. Gas valves are shut off and trains are slowed when an alert is received and confirmed by local acceleration observations (Clinton et al. 2016).

System construction is underway in many places around the world using local/regional networks in addition to a global smartphone system. China is beginning the implementation phase of a national system that will initially focus on four regions. A total investment of $280 billion has been made to install 15,000 sensors across earthquake-prone regions and deliver public alerts (Li 2018). Also, the high-speed rail is in the process of developing independent systems (Lu et al. 2016). Chile has been expanding its seismic and geodetic networks since the M8.8 offshore of central Chile in 2010. It has been testing the ElarmS (Kuyuk et al. 2014) and FinDer (Böse et al. 2017) algorithms as well as experimenting with the deployment of modified smartphones to collect geodetic data (Minson et al. 2015). Costa Rica, El Salvador, and Nicaragua have been building capacity in EEW and are testing the Virtual Seismologist (VS) (Cua & Heaton 2007) and FinDer (Böse et al. 2017) algorithms. Israel is currently constructing an improved national seismic network with the specific goal of delivering alerts. It is currently testing the ElarmS algorithm on the growing network (Nof & Allen 2016). The Irpinia region of Italy is running the PRESTo point source algorithm with the goal of delivering alerts in Naples and the surrounding region (Satriano et al. 2010). Switzerland has a high-quality national seismic network and is continuing testing and development of the VS (Cua & Heaton 2007) and FinDer (Böse et al. 2017) algorithms.

Finally, the MyShake project (**https://myshake.berkeley.edu/**) has developed the capability to detect earthquakes using private/personal smartphones with the goal of collecting earthquake data from their global smartphone network and delivering alerts to users (Kong et al. 2016b). The use of this nontraditional sensor network makes it possible to provide alerts in earthquake-prone regions where there are smartphones (i.e., wherever there are people). With over 300,000 downloads to date, the system has detected over 800 earthquakes and demonstrated the end-to-end capability to create alerts (Kong et al. 2016a). To issue alerts in multiple regions around the world, the number of users will need to increase significantly, but the hope is that once the system starts issuing alerts, many more people will download the app and participate.

**PRESTo:** earthquake early warning algorithm using P-wave data to estimate the location and magnitude of an earthquake

**MyShake:** global smartphone seismic network that detects earthquake shaking, records ground acceleration time series, and generates earthquake alerts using private/personal smartphones

## 3. RECENT ADVANCES

As previously noted, the bulwark of EEW for the last 30 years has been the point source algorithm. Point source algorithms continue to be improved upon, and new approaches such as finite faulting

and ground motion methods have matured. In this section we review these and other relevant methodological advances.

**Gutenberg algorithm:** uses frequency content of the P-wave at a single site to estimate the likely distance to the earthquake source and its magnitude

**Integrated particle filter (IPF):** method using information about stations triggering on a seismic arrival to determine if one or more earthquakes are underway

## 3.1. Improvements to Point Source Algorithms

Timely alerts are the most important attribute of point source methods. For fast alerts network density exerts a first-order control on how quickly an earthquake will be detected and thus the size of the blind zone where no alert is possible (Kuyuk & Allen 2013). However, as noted in Section 1.2 and **Figure 1**, there is a trade-off, introduced by the details of the algorithm, between magnitude uncertainty (and thus ground motion uncertainty) and speed of the alert. Broadly speaking, algorithms that require several stations to trigger before issuing an alert will experience fewer false alerts and produce more robust source and ground motion estimates. However, they will be slower. Single station algorithms, conversely, will be faster but will be more error prone both by having larger uncertainty in their estimate of magnitude and by being more susceptible to false alerts. Several heuristics have been proposed (e.g., Böse et al. 2009) to improve the performance of single station event detection with modest success. A more robust approach was proposed by Meier et al. (2015), who used a novel filterbank technique. This significantly reduces the uncertainty by exploiting more features of the early onset waveforms. The filterbank outputs are used for joint Bayesian estimation of the magnitude and source-to-station distance. By inferring these parameters jointly, this proposed Gutenberg algorithm relies on the notion that large amplitudes at high frequencies will be observed only if the source-to-station distance is short. Similarly, high amplitudes at long periods should be observed only if the magnitude is large. The Gutenberg algorithm produces better estimates with only one to two stations than traditional onsite methods and thus can speed up the first alert and reduce the blind zone substantially.

Meier et al. (2015) also suggested that prior information such as proximity to known fault structures or areas of recent seismicity could be used as a beneficial constraint; Yin et al. (2018) showed exactly that. They combined traditional waveform features with epidemic-type aftershock sequence seismicity forecast in a Bayesian framework and showed that misidentification of nonearthquake signals was greatly reduced, especially during periods of substantial activity such as during swarms or mainshock-aftershock sequences. Suboptimal performance of EEW systems during aftershock sequences is an important open problem. In the days following the M9 Tohoku-oki earthquake, due to the rich aftershock sequence, 63% of the 70 warnings issued were false warnings where the intensity was overestimated by two intensity levels (Liu & Yamada 2014). This is due to events occurring close together in time being misidentified as a single event. Liu & Yamada (2014) proposed a novel integrated particle filter (IPF) method to separate such events. The IPF algorithm is a Bayesian estimator that uses information from both triggered and nontriggered stations. Data from nontriggered stations, often referred to as not-yet-arrived data, are critical for the success of the IPF algorithm. During the 2016 M7.2 Kumamoto earthquake, the IPF algorithm showed good offline performance, and it is being phased into production by JMA (Kodera et al. 2016).

Other impacts of the M9 Tohoku-oki earthquake relate to the well-documented magnitude saturation experienced by the point source algorithm (Hoshiba & Ozaki 2014), which estimated the event at M8.1. Substantial effort has been invested in approaches that allow more prompt and unsaturated magnitude estimation of large events. A core improvement revolves around developing better approaches for using the evolving features of a waveform rather than fixed-length time windows. Noda & Ellsworth (2016, 2017) studied events in Japan and suggested that by using varying window lengths between 0.5 s and 4 s, convergence to final magnitudes could be substantially accelerated for moderate magnitude events. However, those studies, echoing Hoshiba & Ozaki (2014), found no improvement for the largest magnitude events.

This contrasts with Colombelli et al. (2014) and Colombelli & Zollo (2015). They found more positive results for the same Japanese data set of strong motion recordings. In their approach, in addition to using progressively expanding P-wave windows, they averaged many waveforms over many distances and azimuths together. They found that the growth of this average displacement waveform event exhibited markedly different character for events as large as M9. For events in the M8–8.5 range, such a method would yield useful source parameters 30–40 s after origin time, although for the M9 Tohoku-oki event, this method still underestimated the earthquake at M8.4.

This averaging approach is tricky to apply in real time. As the P-wave time window expands, some stations will not be useful after a certain point because S-wave energy will begin to leak into the parameter estimation. Kodera (2018) proposed an interesting solution to this, showing that through ground motion polarization analysis of borehole sites, it is possible to build a P-detector to measure P-waves on the vertical channels even after the first S-wave onsets. For large earthquakes in Japan, these late-arriving P-waves can be used to track an evolving rupture and provide better intensity estimates with more lead time. One potential limitation is that the P-detector method is likely useful only for borehole sites since free-field stations will be affected by soil response that will degrade the performance.

Other approaches for obtaining timelier unsaturated magnitudes of large events focus on alternative features of ground motion recordings. Noda et al. (2016) showed that magnitude correlates well to the time difference between the S-wave onset and the arrival of the peak high-frequency amplitude in an accelerogram. Importantly, this time is shorter than the source duration. For the M9 Tohoku-oki earthquake, such an approach would have produced an unsaturated magnitude estimate 120 s after origin time. However, by using high-frequency data, the method is susceptible to complexities in the source such as the location of strong motion-generating areas (Asano & Iwata 2012), which can produce anomalously long apparent durations.

Similarly, several researchers have studied the behavior of peak ground displacement (PGD) as measured by a high-rate global positioning system (HR-GPS). Crowell et al. (2013) first noted that for the 2003 M8.3 Tokachi-oki and M9 Tohoku-oki earthquakes, PGD could be a reliable magnitude estimator. Melgar et al. (2015) then expanded the data set to include a number of M8+ events in Chile and M7+ events worldwide and proposed an algorithm for rapid PGD magnitude estimation. PGD does not exhibit magnitude saturation, and it can be used to estimate final magnitudes, depending on network configuration, between one-half and two-thirds of the way through the source process. For example, final magnitudes were obtained after 60 s and 100 s for the M8.8 Maule and M9.0 Tohoku-oki earthquakes. Crowell et al. (2016, 2018b) produced operational prototypes of the PGD magnitude algorithm as part of the ShakeAlert EEW system and for Chile as well.

**Peak ground displacement (PGD):** maximum displacement that occurs at a site during the passage of seismic waves

**High-rate global positioning system (HR-GPS):** high-rate geodetic time series having sample rates of one sample per second or more, providing information about ground displacement

## 3.2. Finite Fault Algorithms

One of the other open challenges in EEW is unsaturated magnitude and ground motion estimation of large events. One potential solution is to explicitly quantify fault finiteness in real time from seismic and geodetic measurements. This is important because a particular location can be far from the hypocenter but close to a strong motion-generating area of a fault, in which cases point source algorithms, when converted to ground motion, will lead to large misestimations of the actual hazard. For example, during the 2011 M9 Tohoku-oki earthquake, shaking in the Kanto region around Tokyo, 350 km from the epicenter, was seriously underpredicted (Hoshiba & Ozaki 2014).

The FinDer algorithm (Böse et al. 2012) estimates fault rupture extent and strike by analyzing the spatial distribution of ground motions in real time. At any given instant FinDer interpolates

**G-larmS:** earthquake early warning algorithm using HR-GPS to estimate the finite extent of the fault rupture and the magnitude

the observed maximum ground motion to produce an image of the maximum observed shaking. FinDer simplifies a potentially complex distribution of shaking by using ground motion thresholds to divide sites into near and far from the rupture. This classification produces a binary image of maximum-observed shaking at a given point in time. FinDer then compares this binary image to previously computed templates of shaking distributions obtained from GMPEs and finds the best-matching template. Each template has an associated fault length, and strike and magnitude are then determined from fault length scaling relationships.

Unlike the point source algorithms, FinDer is not a predictive algorithm. It does not estimate whether an event will grow; rather, it is a real-time ground motion assessment. Although FinDer was initially conceived for large events, modifications to the ground motion thresholds and other parameters have made it suitable for small-magnitude events as well (Böse et al. 2015). With regards to timeliness, if a network is dense enough, FinDer is surprisingly fast, with first alerts often only a few seconds behind point source algorithms (Böse et al. 2017). Indeed, recent demonstrations of FinDer performance for large crustal events such as the M7 Kumamoto earthquake (Böse et al. 2017) showcased the utility of the algorithm. Because it relies on template images of the distribution of ground shaking, FinDer performs at its best when an earthquake occurs within the footprint of the seismic network providing it with data. Böse et al. (2015) added asymmetric or one-sided templates to allow the algorithm to deal with subduction zone earthquakes occurring out of the network. Offline testing during the M9.0 Tohoku-oki earthquake was encouraging. FinDer estimated the event to be M8.5 and 270 km long 160 s after origin time. More rigorous testing is necessary with more large subduction zone events that have one-sided distributions of shaking.

A second class of finite fault algorithm relies on HR-GPS data. Automated static slip inversion was first demonstrated by Crowell et al. (2009), and research into it has been facilitated predominantly by two significant events recorded in real time. First, the M7.2 El Mayor-Cucapah earthquake in northern Mexico was recorded across a large network of GPS stations in Southern California. From these data Allen & Ziv (2011) and Crowell et al. (2012) made the first concrete demonstrations and recommendations of what an operational GPS-enhanced warning would entail. The second significant event was, of course, the 2011 M9 Tohoku-oki earthquake, which was recorded across more than 1,000 HR-GPS stations in Japan. From these data a number of workers noted and demonstrated that had HR-GPS data been used for simplified inversion, then the magnitude saturation problem would have been resolved (Ohta et al. 2012, Wright et al. 2012, Melgar et al. 2013). Knowledge of fault finiteness improves ground motion estimates by allowing one to use more physically realistic estimates of site-to-fault distance. Indeed, for the GPS approaches, Colombelli et al. (2013) showed that not only were magnitude estimates from simplified GPS slip inversions reliable across a large range but also the ground motion estimates from such source models were a substantial improvement over point source–driven calculations. Specifically, in the M9 Tohoku-oki case, the GPS models were available quickly enough to be useful for better ground motion estimates in the Kanto region around Tokyo.

Because of these findings, many algorithms have been proposed and are being tested. Notably, in the United States, three algorithms are undergoing testing and being considered for ShakeAlert (Murray et al. 2018). All of them rely on event notifications or triggers from the seismic system. This is preferred because GPS data can be noisy, and event detection on these waveforms can lead to many false alerts. The first of these three is the G-larmS algorithm (Grapenthin et al. 2014a, 2014b), which, following an event trigger, calculates static slip inversions on a series of predefined geometries that correspond to tectonic domains. For example, within Northern California, it considers slip to be possible on San Andreas fault parallel and conjugate vertical strike slip geometries as well as on blind thrust faults with strike and dip similar to the well-known Mt.

Diablo fault. Another algorithm, G-FAST (Crowell et al. 2016), first computes a moment tensor from the static offsets using the Melgar et al. (2012) method and then attempts the slip inversion on the two nodal planes from the moment tensor and determines that the one that best fits the data is the preferred solution. A third algorithm, BEFORES (Minson et al. 2014), simultaneously estimates slip and the most likely fault geometry using a simplified Bayesian formulation.

Outside the United States, implementation of GPS finite faulting algorithms has begun in Chile, where the G-FAST algorithm is undergoing testing (Crowell et al. 2018b). Similar efforts are underway in Japan. Following the M9 Tohoku-oki earthquake, Ohta et al. (2012) proposed an inversion algorithm that inverts for fault geometry and extent with homogenous slip. They demonstrated convergence to M8.8 within ~150 s of origin time. This detection and inversion algorithm, called REGARD, has begun operational testing with some modifications (Kawamoto et al. 2016, 2017). REGARD consists of two simultaneous inversions. First, a nonlinear inversion of a single rectangular fault loosely constrained to an a priori model of allowed fault orientations is carried out. Concurrently, a linear inversion of a slip distribution model fixed to the assumed subducting plate boundary is performed. The algorithm has been successfully tested for several crustal and subduction zone events.

Testing the performance of GPS algorithms under a variety of circumstances remains challenging. GPS is somewhat insensitive and typically can measure ground motions only for earthquakes larger than M6. As a result, because only a few events occur within the footprint of a given network, retrospective real-time replays of events elsewhere in the world are common. For example, Crowell et al. (2018a) showed that for the very complex M7.8 Kaikoura earthquake, the simplified G-FAST solution was useful for ground motion prediction. Ruhl et al. (2019b) have made available a database of more than 3,000 HR-GPS recordings for 29 large events that can be used by algorithm developers for benchmarks and testing. Indeed, in a follow-up study Ruhl et al. (2019a) used these data and publicly available strong motion recordings to show that the G-larmS algorithm, while slower to converge to the final magnitude, is still fast enough to forecast strong motions. This is because of the protracted nature of the source process and the ability of the algorithm to estimate fault finiteness. For large earthquakes that are expected to occur but for which no example data are available, one possibility is to use scenarios and simulated data. For example, the Cascadia subduction zone is known to produce events up to M9; however, because no instrumental data of any significant megathrust event are available, Melgar et al. (2016) proposed a simulation approach that synthesizes HR-GPS data from kinematic rupture scenarios. Ruhl et al. (2017) used these data to assess the performance of the G-larmS algorithm in the Cascadia subduction zone and, because of that analysis, were able to propose a set of improvements and modifications to the algorithm.

Overall, finite fault algorithms provide a more complete characterization of the source and do not saturate, which results in better ground motion estimates. However, they need observations at many sites and for longer times and thus will always be slower than point source solutions. As a result, they are of limited use at short epicentral distances and can provide actionable information only some distance away from the earthquake origin (**Figure 1**).

**G-FAST:** earthquake early warning algorithm using HR-GPS to estimate the seismic moment tensor and then inverting for slip on the fault plane

**BEFORES:** earthquake early warning algorithm using HR-GPS to simultaneously estimate the most likely fault plane and slip distribution

**Propagation of local undamped motion (PLUM) algorithm:** algorithm using a dense network to measure the ground motion and forward predict likely motion at surrounding sites

### 3.3. Ground Motion–Driven Approaches

A new generation of algorithms has emerged (Hoshiba 2013, Hoshiba & Aoki 2015, Kodera et al. 2018) that avoids estimation of source parameters. These algorithms use physics-driven data assimilation techniques. The core idea is to use the present state of the ground shaking and knowledge of propagation physics to forecast the likely evolution of intensity some short time (<20 s) in the future. Specifically, the propagation of local undamped motion (PLUM) algorithm (Hoshiba & Aoki 2015) has undergone substantial refinement and testing in Japan.

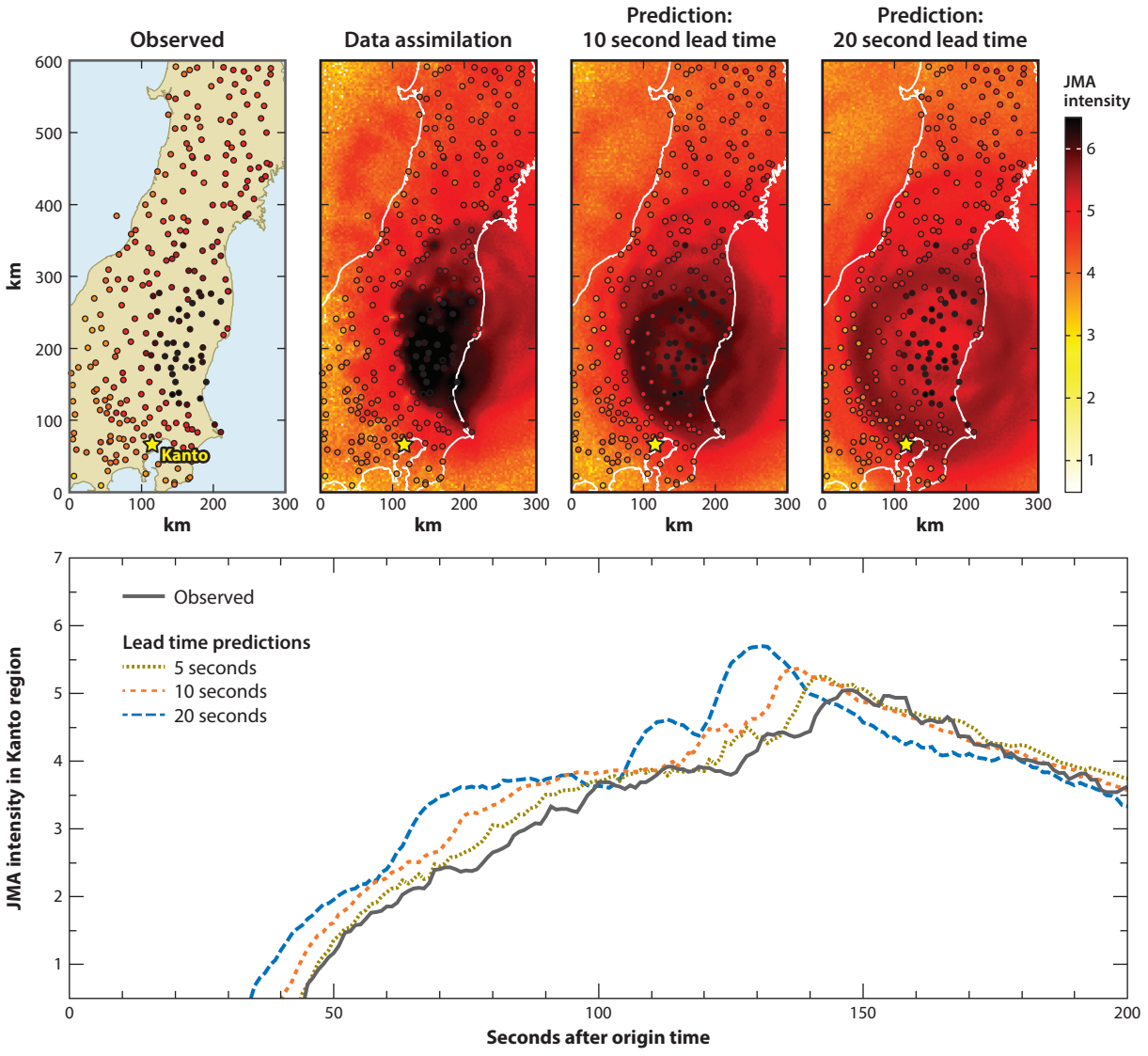


**Figure 3**

Retrospective performance of the PLUM algorithm during the M9 Tohoku-oki earthquake. Shown are the ground motion forecasts available 10 s and 20 s before the onsets of shaking. Abbreviations: JMA, Japan Meteorological Agency; PLUM, propagation of local undamped motion. Figure adapted with permission from Hoshiba & Aoki (2015).

In the PLUM method, first a spatially dense image of the present distribution of intensity is formed. Through data assimilation techniques, this image is forecast into the future using radiative transfer theory. This is a high-frequency ray theoretical approximation that neglects details of the wavefield and is, rather, an estimate of energy propagation. The approximation is chosen because it is far faster than numerical approaches that propagate the full wavefield, so it is more suitable for real-time applications. An example of this procedure for the M9 Tohoku-oki earthquake is shown in **Figure 3**. After an image of the present wavefield is formed, it can be forecast 10 s and 20 s into the future.

The main strength of PLUM is that it does not require any knowledge of the source; it simply assumes that the physics is known to forecast the observed intensities a short time into the future. Like FinDer, PLUM is not a predictive algorithm and cannot anticipate whether a rupture will keep growing. However, by its very nature, it will capture fault finiteness effects if they have been observed in the distribution of ground shaking. Additionally, it can easily handle multiple events in quick succession, such as during early aftershock sequences. It is possible to empirically add site-effect and path-effect corrections, and thus, with short 10- to 20-s lead times, PLUM can provide very accurate intensity forecasts.

Development of the algorithm was driven by the low ground motion forecasts in the Kanto region around Tokyo during the M9 Tohoku-oki earthquake and the many missed alerts in the aftershock sequence. Retrospective testing of this event has shown the desired improved performance (Hoshiba & Aoki 2015). Furthermore, during the more recent 2016 M7 Kumamoto earthquake, PLUM performed well during the mainshock and also during the vigorous aftershock sequence (Kodera et al. 2016). The algorithm is now in real-time operations in Japan (Kodera et al. 2018).

### 3.4. Combining Algorithms

Individual algorithms—point source, finite fault, ground motion driven, and others—all have different strengths and weaknesses. Thus, to achieve the best performance in all possible situations, it is desirable to simultaneously operate several algorithms. The challenge is how to then synthesize, or combine, information from all these disparate sources. Combining earthquake source information from a point source and a finite fault algorithm is not desirable; rather, it is preferable to combine ground motion forecasts. A simple solution proposed by Kodera et al. (2016) is to take the largest intensity estimate from any given algorithm for a particular location. Indeed, in the operational system in Japan, the maximum ground motion from the PLUM and the conventional point source algorithm is taken at any point in time (Kodera et al. 2018). Minson et al. (2017) proposed a more elegant solution. Using a Bayesian formulation, they designed a central decision module that provides a single estimate of shaking by assigning likelihoods to the forecasts of different algorithms by comparing predicted and observed waveform envelopes. In this framework the predictions from many algorithms, even when they have physically incompatible source models such as point source or finite faulting, can be combined (e.g., Ruhl et al. 2019a).

### 3.5. Timeliness and Accuracy of Ground Motion Forecasts

There has been a recent push to systematically evaluate how well shaking intensities of certain levels can be forecast and how large the prediction errors are as a function of time (e.g., Hsu et al. 2016, Meier 2017, Kodera et al. 2018, Minson et al. 2018). Critical to these analyses of ground motion is the concept of an alert threshold, which signifies a user-defined ground motion level at which an action will be triggered. Different thresholds will produce different warning times.

Once a threshold is selected for any particular location, alerts are classified as true or false positives and true or false negatives if the alert threshold was correctly or incorrectly forecast to be exceeded or not. Using this approach Meier (2017) analyzed several thousand waveforms employing a P-wave displacement point source method and a theoretical idealized finite fault algorithm. Meanwhile, Minson et al. (2018) studied point source and finite fault algorithms from theoretical considerations. Both studies concluded that for a high MMI threshold, fewer alerts—both false and correct—will be issued, but the alerts that are issued can have a large proportion of false alarms due to the inherent difficulty in forecasting large intensity ground motions. Ruhl et al. (2019a) extended this approach and conducted a retrospective test of 32 $6 < M < 9$ events worldwide. They

replayed seismic and geodetic data through both point source and finite fault algorithms and quantified the accuracy of ground motion prediction. The study provided the first systematic test of a system on a wide array of real and varied geophysical data. It effectively showed that the addition of the global navigation satellite system (GNSS) finite faulting approach substantially improves the ground motion prediction ability of the system. As the point source algorithm saturates, the GNSS algorithm begins to provide useful information for users who, while further afield from the hypocenter, are still close to the finite fault and experience substantial shaking. Similarly, a low MMI threshold means that alerts are issued more often and the probability that any individual alert is correct is much higher; however, cumulatively, more false alerts are issued.

Recognizing the inherent uncertainty in ground motion estimation, Kodera et al. (2018) proposed that, rather than study the classification on a station-by-station basis, it is preferable to study the accuracy of ground motion prediction over small, spatially averaged geographical areas. In their analysis of events in Japan using the hybrid point source–PLUM method, Kodera et al. (2018) found that PLUM achieves a high prediction score of 90%. This score is given as the proportion of correctly classified true positives and negatives and false positives and negatives for an alert threshold of 3.5 on the JMA intensity scale. The algorithm had warning times between 6 and 35 s.

These quantitative efforts at assessing algorithm performance are important because they are an objective way to measure improvements (or degradation) of a system's performance and to advocate for one algorithm over another. In the United States in particular, a testing and certification platform based on these metrics, and others, is in the process of being standardized (Cochran et al. 2017). However, recall from Section 1 that the kinds of users of an EEW system are varied, and an open problem is that no quantitative research exists on the tolerance of any kind of user to false or missed alerts. So, while we can quantify the seismological performance of a system and set goals for what is and is not acceptable from a system performance standpoint, we lack the information to combine these findings with quantitative assessments of user tolerance.

### 3.6. The Question of Determinism

The question of source determinism, which has been debated since modern EEW was proposed, continues to be debated today. Determinism means when, within a potentially minutes-long rupture process, a very large earthquake can be distinguished from a large one. For EEW it is an important issue because it defines the minimum theoretical time at which the hazard (ground shaking) can be characterized. One end member is strong determinism, where the nucleation process is different between earthquakes of eventually different final magnitudes (e.g., Ellsworth & Beroza 1995). In this view a few seconds of observation can be used to identify events (e.g., Olson & Allen 2005). Colombelli et al. (2014) suggested that the evolution of displacements imaged by dense strong motion networks in Japan was strong evidence of this. However, Meier et al. (2016), also from an analysis of strong motion data, found that nucleation is likely a universal process and thus independent of final magnitude. Hoshiba & Iwakiri (2011) analyzed strong motion records from the first 30 s of the M9 Tohoku-oki earthquake and found no difference between it and events of smaller magnitude originating in the same region, echoing previous findings from Rydelek & Horiuchi (2006). Meier et al. (2017) further analyzed several large databases of teleseismically determined STFs and contended that, at least in the first third, there are no differences in the STFs of large and very large events. From an analysis of the same STFs and near-field GPS, a more nuanced view was proposed by Melgar & Hayes (2017), who suggested that there is weak determinism. In this view nucleation is a magnitude-independent process, but shortly thereafter (~10 s), a self-similar slip pulse develops whose properties (rise time and pulse width) are

diagnostic of the eventual final magnitude. Goldberg et al. (2018) analyzed many HR-GPS records in Japan and reached similar conclusions.

## 4. FUTURE OUTLOOK

Throughout Section 3 we described the incremental improvements made in the last ~10 years to EEW systems. Despite these advances, the basic concepts of the EEW paradigm demonstrated by the first operational systems (e.g., Nakamura 1988, Espinosa-Aranda et al. 1995) regarding both sensors and algorithms have remained largely unchanged. In this section we highlight research that could impact, at its core, how EEW is realized.

EEW has relied strictly on onshore networks. However, in many subduction zone environments, nucleation of large, damaging events occurs predominantly offshore. Thus, there has been a push for real-time telemetered ocean bottom networks. The largest effort to date is that of the S-net network in Japan (Kanazawa et al. 2016), which consists of more than 800 km of fiber-optic cable covering the Japan trench with 150 nodes, or observatories, spaced roughly every 30 km. Each node contains absolute-pressure, strong motion, broadband, and short-period sensors. Although smaller in scope, similar real-time cables exist at the Cascadia subduction zone (**Figure 4**) on both the Canadian (Barnes et al. 2011) and the US (Tréhu et al. 2018) portions of the system.

Such real-time cabled observatories have the potential to speed up detection of unfolding events and thus warning; however, they come at a cost that is significantly greater than their onshore counterparts'. Techniques to deploy and maintain infrastructure like this are still evolving. The ocean bottom is a challenging environment. Both the cables and the observing nodes need to be buried or made trawl resistant to protect them from fishing activities. Additionally, there are numerous noise sources such as bottom currents and internal waves that can make the data difficult to use, particularly at long periods (Webb 1998). However, research has shown that it is possible to correct and account for the noise (e.g., Bell et al. 2014), and thus it is becoming possible to reliably use real-time seafloor data. Offshore networks have intrinsic value not just for these hazards applications but also for basic science exploration, so it is likely that they will continue to expand in the coming decades and allow for better and more timely alerts, especially for the largest events.

Onshore, it has been shown that a significant portion of the delay between detection and characterization of an event and issuance of the first alert is directly related to the density of the sensing network (e.g., Kuyuk & Allen 2013, Ruhl et al. 2017). Simply put, with a sparser network, the blind zone is larger. Observatory-grade equipment is expensive and thus limits the growth of most networks. One potential approach is to supplement traditional sensor networks with low-cost accelerometers. Substantial progress has been made in MEMSs, and their noise characteristics and sensitivity have been well studied. They are suitable for local monitoring (Evans et al. 2014, Saunders et al. 2016). MEMS accelerometers are a fraction of the cost of traditional inertial seismometers and thus could be deployed to augment a network's density. Chung et al. (2015) showed that the sensors can be used by currently existing point source algorithms, and Clayton et al. (2015) deployed more than 500 MEMS devices in the Los Angeles region. In Taiwan 543 MEMS sensors supplement the traditional network (Chen et al. 2015).

Despite these improvements, large MEMS deployments still face some of the same challenges as traditional seismic stations. Permits and permissions need to be secured to deploy devices, and telemetry paths need to be built. Thus, while MEMSs are cheap, their maintenance might not be any less costly than that of a traditional network. Perhaps the most exciting development in low-cost sensing comes from the potential to use mobile phones as seismometers. Most smartphones today carry onboard a three-component MEMS accelerometer of sufficient quality to detect

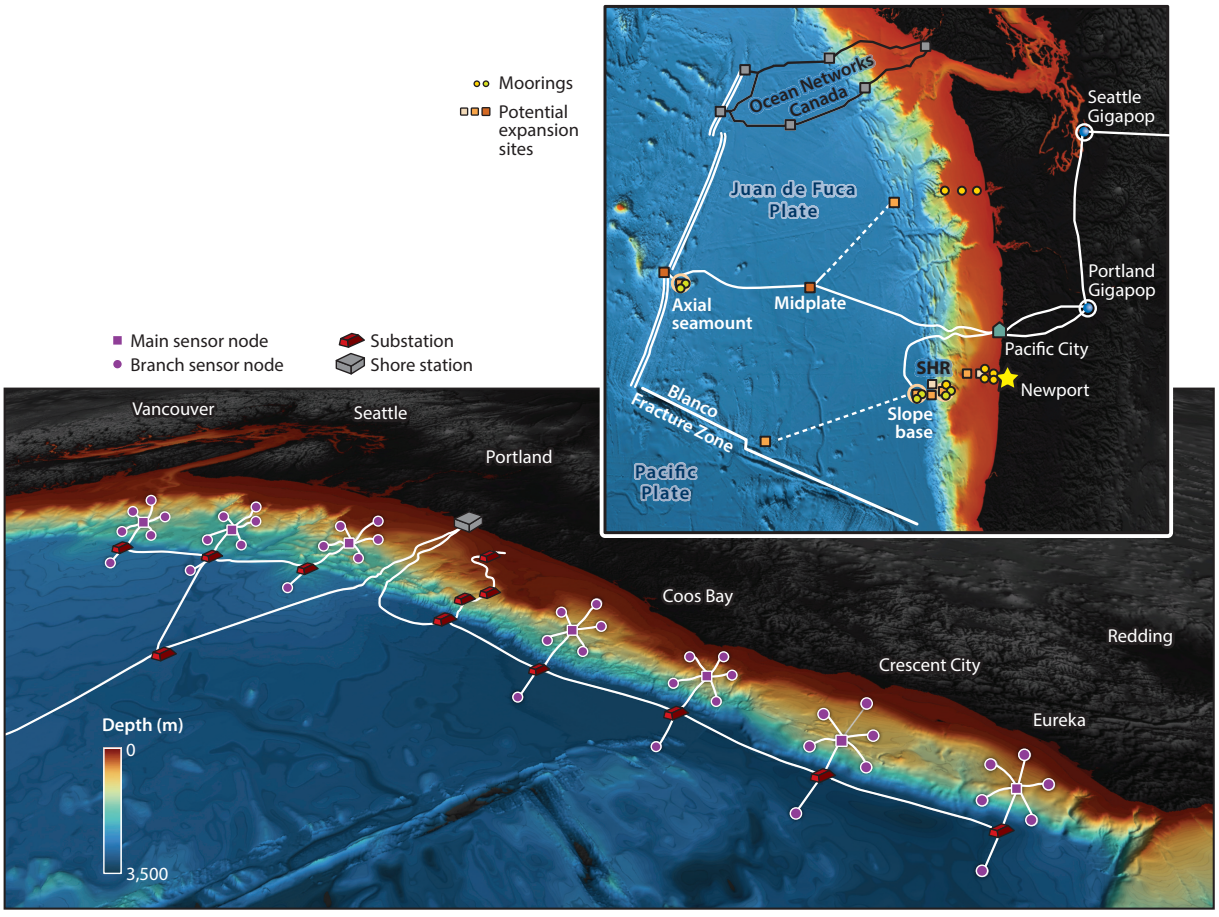


**Figure 4**

(*Top*) Current state of seafloor networks in the Cascadia subduction zone. (*Bottom*) Conceptual sketch of a potential expansion to the seafloor infrastructure. Abbreviation: SHR, Southern Hydrate Ridge. Figure adapted with permission from original by Will Wilcock and Hunter Hadaway, University of Washington.

moderate and large events at local to regional distances (Kong et al. 2016b). Indeed, if the mobile phone is at rest, the onboard sensors are good enough to observe P-waves and thus are suitable for EEW. Kong et al. (2016a,b) demonstrated the ability to collect and analyze data from the phones in real time with minimal impact to the user's phone in terms of battery consumption or processor use. Additionally, Kong et al. (2016b) demonstrated with an artificial neural network that it is possible to reliably separate human signals from earthquake signals recorded on the phone. Kong et al. (2016a) further demonstrated how the data can be used for EEW. In related work, Minson et al. (2015) showed through simulations of large events that the GPS chips in modern smartphones could also be useful for warning. Because there are more than 2 billion smartphone users around the world, the ability to harness them for warning is an exciting prospect.

By and large, however, EEW systems continue to rely on traditional inertial seismometers. There is potential for contributions from other geophysical sensors. Barbour & Crowell (2017) showed that strainmeters, which measure elastodynamic strain over a very broad frequency range, could be reliably used for rapid source characterization. While they conducted their analysis on

onshore instruments, their findings are interesting because it is possible that strain will be one of the preferred geodetic measurements in future offshore networks. Another interesting result relating to geodesy was described by Montagner et al. (2016). They found that a gravity signal preceding the P-wave was detected by the Kamioka superconducting gravimeter during the M9 Tohoku-oki earthquake. During the rupture process, slip on a fault redistributes mass within the crust, as do the radiated elastic waves, and thus a gravity perturbation is expected. Montagner et al. (2016) and Vallée et al. (2017) produced a theoretical formulation for such transient elastogravity signals. For the M9 Tohoku-oki earthquake, Vallée et al. (2017) showed that the postulated gravity perturbations preceding the P-wave arrivals could indeed be observed on broadband seismometers (**Figure 5**). These findings are encouraging because gravity perturbations propagate at the speed of light, so a system that uses such measurements operationally would be substantially faster by eliminating the travel-time delay from P-waves traveling from source to site. However, even for the M9 Tohoku-oki earthquake, the perturbations were quite small (~1 nm/s$^2$), and thus, only the largest of events will generate signals that could be measured with the current generation of broadband sensors.

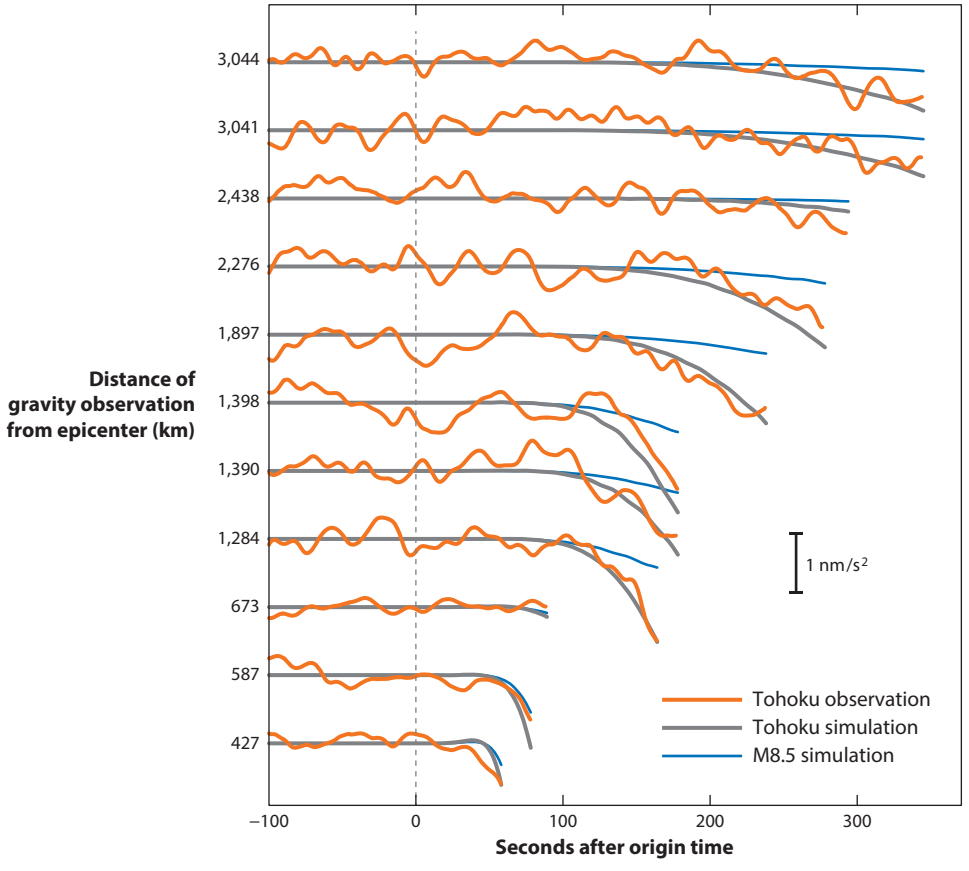


**Figure 5**

Agreement between observed and simulated elastogravity acceleration signals for the M9 Tohoku-oki earthquake. The simulation for a fictitious M8.5 earthquake shows large amplitude differences, directly illustrating the magnitude determination potential existing in these signals. The waveforms are truncated before P-wave arrivals. Figure adapted with permission from Vallée et al. (2017).

**Machine learning (ML) algorithm:** algorithm designed to recognize patterns in data to classify them or predict future actions or observations without a physical model

Finally, another broad and exciting avenue of research for future EEW systems comes from modern data science and specifically from machine learning (ML). Modern seismic equipment will sense other environmental signals, both anthropogenic and otherwise. From time to time, one of these nonearthquake signals will trigger an individual station. If there are many stations, especially in noisy urban environments, the potential for several of these false triggers to occur close to each other in space and time and be associated into a false alarm is non-negligible. One solution is to introduce new algorithms for signal discrimination. Perol et al. (2018) demonstrated that a convolutional neural network (CNN) algorithm, often referred to as deep learning, could be used for detection and location. Ross et al. (2018) used the CNN algorithm to identify P-waves, S-waves, and nonevent signals in continuous data. The performance is far better than with traditional triggering and detection algorithms and, if applied to real-time EEW networks, will substantially reduce false alerts. It is easy to envision other as-yet-to-be-explored ML applications. ML algorithms could be trained to recognize magnitude, location, and other source features directly from the waveforms themselves, forgoing the need for a magnitude regression. Additionally, as in the PLUM method, images of ground shaking can be formed and used to train ML algorithms in a predictive sense such that when the next earthquake occurs, an ML algorithm can forecast the most likely evolution of the present wavefield some time into the future.

## 5. CONCLUSIONS

Earthquakes can be major catastrophic events and disrupt people's lives in very significant, sudden, and uncontrollable ways. EEW is one relatively new tool to help reduce an earthquake's impact and provide people with an ability to take back some control by reacting to the warning. Public interest in EEW has driven the rapid development of methodologies over the last decade, which is in turn driving a deeper understanding of earthquake physics as we develop improved models of the earthquake process to better predict ground shaking. At the same time, EEW leads to the deployment of new geophysical networks providing the data for EEW and further research and development. This process can be observed in the countries that currently deliver public alerts (Mexico, Japan, South Korea, and Taiwan), the countries delivering limited alerts (India, Romania, Turkey, and the United States), and the many additional regions developing systems.

The algorithms in use fall into four categories. Point source algorithms are in use in all regional systems and provide earthquake information in a few seconds. In larger earthquakes ($M > 7$), there is time for finite source algorithms to provide unsaturated magnitude estimates and describe the fault geometry, both of which lead to more accurate alerts. GMMs provide the most accurate estimate of forthcoming shaking by forward predicting observed shaking, but they are limited to a few seconds of warning. Finally, onsite approaches are the simplest in that they use a sensor at one location to warn the same location, but they have limited accuracy and warning time.

EEW systems several decades from now will evolve out of what exists today but will likely be substantially different. Systems will be amphibious and cross shorelines. More diverse geophysical observations will exist, including not just HR-GPS but also perhaps strainmeters and pressure or acoustic sensors on the seafloor. Observatory-grade sensors will form a backbone network supplemented by MEMS accelerometers in key areas, perhaps surrounding major fault lines, and by millions of mobile phones in urban environments. ML algorithms will more promptly discriminate between myriad environmental signals and correctly identify the onsets of significant events from all these disparate data. Other ML algorithms will classify, from these onset signals, the characteristics of the event and combine that with information of the present state of the wavefield to make forecasts of the likely intensities of shaking some time into the future. Alerts will be tailored according to the level of shaking a geographic region is likely to experience and will be

disseminated through multiple communication channels to millions of people with minimal lag and with simple, easy-to-digest messages. Automated systems will act to secure critical infrastructure, lifelines, and transportation systems, substantially reducing the risk of post-earthquake hazards such as fire. In such a future the benefits of EEW will extend beyond the immediate aftermath of a significant earthquake. A modern EEW system will increase resiliency and allow a society to bounce back to its pre-event condition far faster than it would have otherwise.

## DISCLOSURE STATEMENT

R.M.A. has received research funding from the Gordon and Betty Moore Foundation and state and federal agencies for EEW, holds a patent on the use of smartphones for EEW, and has advocated for the implementation of EEW around the world. D.M. has received research funding from state and federal agencies for EEW and advocated for implementation.

## ACKNOWLEDGMENTS

Much assistance was provided from colleagues around the world in compiling this review. In particular we thank John Clinton, Brendan Crowell, Mitsuyuki Hoshiba, Qingkai Kong, Ashok Kumar, Young-Woo Kwon, Yih-Min Wu, and Masumi Yamada. Original versions of figures were provided by Martin Vallée, Will Wilcock, and Hunter Hadaway. Funding was provided for R.M.A. by the Gordon and Betty Moore Foundation through grants GBMF3024 and GBMF5230 to UC Berkeley and by US Geological Survey grant G17AC00346.

## LITERATURE CITED

Allen RM. 2011. Earthquakes, early and strong motion warning. In *Encyclopedia of Solid Earth Geophysics*, ed. HK Gupta, pp. 226–33. Boston: Springer

Allen RM, Cochran ES, Huggins T, Miles S, Otegui D. 2017. Quake warnings, seismic culture. *Science* 358:1111

Allen RM, Cochran ES, Huggins T, Miles S, Otegui D. 2018. Lessons from Mexico's earthquake early warning system. *Eos Trans. AGU* 99

Allen RM, Gasparini P, Kamigaichi O, Böse M. 2009. The status of earthquake early warning around the world: an introductory overview. *Seismol. Res. Lett.* 80(5):682–93

Allen RM, Kanamori H. 2003. The potential for earthquake early warning in southern California. *Science* 300:786–89

Allen RM, Ziv A. 2011. Application of real-time GPS to earthquake early warning. *Geophys. Res. Lett.* 38(16):L16310

Asano K, Iwata T. 2012. Source model for strong ground motion generation in the frequency range 0.1–10 Hz during the 2011 Tohoku earthquake. *Earth Planets Space* 64:6

Atik LA, Abrahamson N, Bommer JJ, Scherbaum F, Cotton F, Kuehn N. 2010. The variability of ground-motion prediction models and its components. *Seismol. Res. Lett.* 81(5):794–801

Barbour AJ, Crowell BW. 2017. Dynamic strains for earthquake source characterization. *Seismol. Res. Lett.* 88(2A):354–70

Barnes CR, Best MM, Pautet L, Pirenne B. 2011. Understanding Earth–ocean processes using real-time data from NEPTUNE, Canada's widely distributed sensor networks, northeast Pacific. *Geosci. Can.* 38(1):21–30

Bell SW, Forsyth DW, Ruan Y. 2014. Removing noise from the vertical component records of ocean-bottom seismometers: results from year one of the Cascadia Initiative. *Bull. Seismol. Soc. Am.* 105(1):300–13

Böse M, Felizardo C, Heaton TH. 2015. Finite-fault rupture detector (FinDer): going real-time in Californian ShakeAlert warning system. *Seismol. Res. Lett.* 86(6):1692–704

Böse M, Hauksson E, Solanki K, Kanamori H, Heaton T. 2009. A new trigger criterion for improved real-time performance of onsite earthquake early warning in southern California. *Bull. Seismol. Soc. Am.* 99:897–905

Böse M, Heaton TH, Hauksson E. 2012. Real-time finite fault rupture detector (FinDer) for large earthquakes. *Geophys. J. Int.* 191(2):803–12

Böse M, Smith DE, Felizardo C, Meier MA, Heaton TH, Clinton JF. 2017. FinDer v. 2: improved real-time ground-motion predictions for M2–M9 with seismic finite-source characterization. *Geophys. J. Int.* 212(1):725–42

Cauzzi C, Behr Y, Guenan TL, Douglas J, Auclair S, et al. 2016. Earthquake early warning and operational earthquake forecasting as real-time hazard information to mitigate seismic risk at nuclear facilities. *Bull. Earthq. Eng.* 14:2495–512

Chamoli BP, Kumar A, Chen D-Y, Gairola A, Jakka RS, et al. 2019. A prototype earthquake early warning system for northern India. *J. Earthq. Eng.* In press

Chen DY, Wu YM, Chin TL. 2015. Incorporating low-cost seismometers into the Central Weather Bureau seismic network for earthquake early warning in Taiwan. *Terr. Atmos. Ocean. Sci.* 26(5):503–13

Chung AI, Cochran ES, Kaiser AE, Christensen CM, Yildirim B, Lawrence JF. 2015. Improved rapid magnitude estimation for a community-based, low-cost MEMS accelerometer network. *Bull. Seismol. Soc. Am.* 105(3):1314–23

Chung AI, Henson I, Allen RM. 2019. Optimizing earthquake early warning performance: ElarmS-3. *Seismol. Res. Lett.* 90(2A):727–43

Clayton RW, Heaton T, Kohler M, Chandy M, Guy R, Bunn J. 2015. Community seismic network: a dense array to sense earthquake strong motion. *Seismol. Res. Lett.* 86(5):1354–63

Clinton J, Zollo A, Mărmureanu A, Zulfikar C, Parolai S. 2016. State-of-the art and future of earthquake early warning in the European region. *Bull. Earthq. Eng.* 14(9):2441–58

Cochran ES, Kohler MD, Given DD, Guiwits S, Andrews J, et al. 2017. Earthquake early warning ShakeAlert system: testing and certification platform. *Seismol. Res. Lett.* 89(1):108–17

Colombelli S, Allen RM, Zollo A. 2013. Application of real-time GPS to earthquake early warning in subduction and strike-slip environments. *J. Geophys. Res. Solid Earth* 118(7):3448–61

Colombelli S, Zollo A. 2015. Fast determination of earthquake magnitude and fault extent from real-time P-wave recordings. *Geophys. J. Int.* 202(2):1158–63

Colombelli S, Zollo A, Festa G, Picozzi M. 2014. Evidence for a difference in rupture initiation between small and large earthquakes. *Nat. Commun.* 5:3958

Cooper JD. 1868. *Earthquake indicator*. San Franc. Bull. San Franc. Publ. Co., San Francisco, CA

Crowell BW, Bock Y, Melgar D. 2012. Real-time inversion of GPS data for finite fault modeling and rapid hazard assessment. *Geophys. Res. Lett.* 39(9):L09305

Crowell BW, Bock Y, Squibb MB. 2009. Demonstration of earthquake early warning using total displacement waveforms from real-time GPS networks. *Seismol. Res. Lett.* 80(5):772–82

Crowell BW, Melgar D, Bock Y, Haase JS, Geng J. 2013. Earthquake magnitude scaling using seismogeodetic data. *Geophys. Res. Lett.* 40(23):6089–94

Crowell BW, Melgar D, Geng J. 2018a. Hypothetical real-time GNSS modeling of the 2016 $M_w$ 7.8 Kaikōura earthquake: perspectives from ground motion and tsunami inundation prediction. *Bull. Seismol. Soc. Am.* 108:1736–45

Crowell BW, Schmidt DA, Bodin P, Vidale JE, Baker B, et al. 2018b. G-FAST earthquake early warning potential for great earthquakes in Chile. *Seismol. Res. Lett.* 89(2A):542–56

Crowell BW, Schmidt DA, Bodin P, Vidale JE, Gomberg J, et al. 2016. Demonstration of the Cascadia G-FAST geodetic earthquake early warning system for the Nisqually, Washington, earthquake. *Seismol. Res. Lett.* 87(4):930–43

Cua G, Heaton T. 2007. The virtual seismologist (VS) method: a Bayesian approach to earthquake early warning. In *Earthquake Early Warning Systems*, ed. P Gasparini, G Manfredi, J Zschau, pp. 85–132. Berlin: Springer

Cuéllar A, Espinosa-Aranda JM, Suarez R, Ibarrola G, Uribe A, et al. 2014. The Mexican seismic alert system (SASMEX): its alert signals, broadcast results and performance during the M 7.4 Punta Maldonado

earthquake of March 20th, 2012. In *Early Warning for Geological Disasters*, ed. F Wenzel, Z Zschau, pp. 71–87. Berlin: Springer-Verlag

Cuéllar A, Suarez G, Espinosa-Aranda J. 2018. A fast earthquake early warning algorithm based on the first 3 s of the P-wave coda. *Bull. Seismol. Soc. Am.* 108:2068–79

Ellsworth WL, Beroza GC. 1995. Seismic evidence for an earthquake nucleation phase. *Science* 268(5212):851–55

Espinosa-Aranda JM, Jimenez A, Ibarrola G, Alcantar F, Aguilar A, et al. 1995. Mexico City seismic alert system. *Seismol. Res. Lett.* 66:42–52

Evans JR, Allen RM, Chung AI, Cochran ES, Guy R, et al. 2014. Performance of several low-cost accelerometers. *Seismol. Res. Lett.* 85(1):147–58

Given DD, Cochran ES, Heaton T, Hauksson E, Allen RM, et al. 2014. *Technical implementation plan for the ShakeAlert production system—an earthquake early warning system for the West Coast of the United States*. Open-File Rep. 2014-1097, US Geol. Surv., Reston, VA. **https://doi.org/10.3133/ofr20141097**

Goldberg DE, Melgar D, Bock Y, Allen RM. 2018. Geodetic observations of weak determinism in rupture evolution of large earthquakes. *J. Geophys. Res. Solid Earth* 123:9950–62

Grapenthin R, Johanson IA, Allen RM. 2014a. Operational real-time GPS-enhanced earthquake early warning. *J. Geophys. Res. Solid Earth* 119(10):7944–65

Grapenthin R, Johanson IA, Allen RM. 2014b. The 2014 $M_w$ 6.0 Napa earthquake, California: observations from real-time GPS-enhanced earthquake early warning. *Geophys. Res. Lett.* 41(23):8269–76

Hoshiba M. 2013. Real-time prediction of ground motion by Kirchhoff Fresnel boundary integral equation method: extended front detection method for earthquake early warning. *J. Geophys. Res. Solid Earth* 118:1038–50

Hoshiba M. 2014. Review of the nationwide earthquake early warning in Japan during its first five years. In *Earthquake Hazard, Risk, and Disasters*, ed. JF Shroder, M Wyss, pp. 505–29. Waltham, MA: Academic

Hoshiba M, Aoki S. 2015. Numerical shake prediction for earthquake early warning: data assimilation, real-time shake mapping, and simulation of wave propagation. *Bull. Seismol. Soc. Am.* 105:1324–38

Hoshiba M, Iwakiri K. 2011. Initial 30 seconds of the 2011 off the Pacific coast of Tohoku earthquake ($M_w$ 9.0)—amplitude and $\tau_c$ for magnitude estimation for earthquake early warning. *Earth Planets Space* 63:553–57

Hoshiba M, Ozaki T. 2014. Earthquake early warning and tsunami warning of the Japan Meteorological Agency, and their performance in the 2011 off the Pacific coast of Tohoku earthquake (M9.0). In *Early Warning for Geological Disasters*, ed. F Wenzel, J Zschau, pp. 1–28. Berlin: Springer-Verlag

Hsu TY, Lin PY, Wang HH, Chiang HW, Chang YW, et al. 2018. Comparing the performance of the NEEWS earthquake early warning system against the CWB system during the 6 February 2018 $M_w$ 6.2 Hualien earthquake. *Geophys. Res. Lett.* 45:6001–7

Hsu TY, Wang HH, Lin PY, Lin CM, Kuo CH, Wen KL. 2016. Performance of the NCREE's on-site warning system during the 5 February 2016 $M_w$ 6.53 Meinong earthquake. *Geophys. Res. Lett.* 43:8954–59

Johnson L, Rabinovici S, Kang G, Mahin SA. 2016. *California earthquake early warning system benefit study*. CSSC Publ.16-04 PEER Rep. 2016/06, Pac. Earthq. Eng. Res. Cent., Berkeley, CA

Kanazawa T, Uehira K, Mochizuki M, Shinbo T, Fujimoto H, et al. 2016. *S-NET project, cabled observation network for earthquakes and tsunamis*. Paper presented at the 9th Conference in the SubOptic Series, Dubai, Apr. 18–21

Kawamoto S, Hiyama Y, Ohta Y, Nishimura T. 2016. First result from the GEONET real-time analysis system (REGARD): the case of the 2016 Kumamoto earthquakes. *Earth Planets Space* 68(1):190

Kawamoto S, Ohta Y, Hiyama Y, Todoriki M, Nishimura T, et al. 2017. REGARD: a new GNSS-based real-time finite fault modeling system for GEONET. *J. Geophys. Res. Solid Earth* 122(2):1324–49

Kodera Y. 2018. Real-time detection of rupture development: earthquake early warning using *P* waves from growing ruptures. *Geophys. Res. Lett.* 45(1):156–65

Kodera Y, Saitou J, Hayashimoto N, Adachi S, Morimoto M, et al. 2016. Earthquake early warning for the 2016 Kumamoto earthquake: performance evaluation of the current system and the next-generation methods of the Japan Meteorological Agency. *Earth Planets Space* 68(1):202

Kodera Y, Yamada Y, Hirano K, Tamaribuchi K, Adachi S, et al. 2018. The propagation of local undamped motion (PLUM) method: a simple and robust seismic wavefield estimation approach for earthquake early warning. *Bull. Seismol. Soc. Am.* 108(2):983–1003

Kohler M, Cochran E, Given D, Guiwits S, Neuhauser D, et al. 2017. Earthquake early warning ShakeAlert system: West Coast wide production prototype. *Seismol. Res. Lett.* 89(1):99–107

Kong Q, Allen RM, Schreier L. 2016a. MyShake: initial observations from a global smartphone seismic network. *Geophys. Res. Lett.* 43(18):9588–94

Kong Q, Allen RM, Schreier L, Kwon YW. 2016b. MyShake: a smartphone seismic network for earthquake early warning and beyond. *Sci. Adv.* 2(2):e1501055

Kuyuk HS, Allen RM. 2013. Optimal seismic network density for earthquake early warning: a case study from California. *Seismol. Res. Lett.* 84(6):946–54

Kuyuk HS, Allen RM, Brown H, Hellweg M, Henson I, Neuhauser D. 2014. Designing a network-based earthquake early warning algorithm for California: ElarmS-2. *Bull. Seismol. Soc. Am.* 104:162–73

Li S. 2018. Approaching earthquake early-warning. *Overv. Disaster Prev.* 2:14–24

Liu A, Yamada M. 2014. Bayesian approach for identification of multiple events in an early warning system. *Bull. Seismol. Soc. Am.* 104(3):1111–21

Lu C, Zhou L, Zhang Z. 2016. Research and test on China high-speed railway earthquake early-warning system. *Sci. Technol. Rev.* 34(18):258–64

Mărmureanu A, Ionescu C, Cioflan CO. 2010. Advanced real-time acquisition of the Vrancea earthquake early warning system. *Soil Dyn. Earthq. Eng.* 31:163–69

Meier MA. 2017. How "good" are real-time ground motion predictions from earthquake early warning systems? *J. Geophys. Res. Solid Earth* 122(7):5561–77

Meier MA, Ampuero JP, Heaton TH. 2017. The hidden simplicity of subduction megathrust earthquakes. *Science* 357(6357):1277–81

Meier MA, Heaton T, Clinton J. 2015. The Gutenberg algorithm: evolutionary Bayesian magnitude estimates for earthquake early warning with a filter bank. *Bull. Seismol. Soc. Am.* 105(5):2774–86

Meier MA, Heaton T, Clinton J. 2016. Evidence for universal earthquake rupture initiation behavior. *Geophys. Res. Lett.* 43(15):7991–96

Melgar D, Bock Y, Crowell BW. 2012. Real-time centroid moment tensor determination for large earthquakes from local and regional displacement records. *Geophys. J. Int.* 188(2):703–18

Melgar D, Crowell BW, Bock Y, Haase JS. 2013. Rapid modeling of the 2011 Mw 9.0 Tohoku-Oki earthquake with seismogeodesy. *Geophys. Res. Lett.* 40(12):2963–68

Melgar D, Crowell BW, Geng J, Allen RM, Bock Y, et al. 2015. Earthquake magnitude calculation without saturation from the scaling of peak ground displacement. *Geophys. Res. Lett.* 42(13):5197–205

Melgar D, Hayes GP. 2017. Systematic observations of the slip pulse properties of large earthquake ruptures. *Geophys. Res. Lett.* 44(19):9691–98

Melgar D, LeVeque RJ, Dreger DS, Allen RM. 2016. Kinematic rupture scenarios and synthetic displacement data: an example application to the Cascadia subduction zone. *J. Geophys. Res. Solid Earth* 121(9):6658–74

Minson SE, Brooks BA, Glennie CL, Murray JR, Langbein JO, et al. 2015. Crowdsourced earthquake early warning. *Sci. Adv.* 1(3):e1500036

Minson SE, Meier MA, Baltay AS, Hanks TC, Cochran ES. 2018. The limits of earthquake early warning: timeliness of ground motion estimates. *Sci. Adv.* 4(3):eaaq0504

Minson SE, Murray JR, Langbein JO, Gomberg JS. 2014. Real-time inversions for finite fault slip models and rupture geometry based on high-rate GPS data. *J. Geophys. Res. Solid Earth* 119(4):3201–31

Minson SE, Wu S, Beck JL, Heaton TH. 2017. Combining multiple earthquake models in real time for earthquake early warning. *Bull. Seismol. Soc. Am.* 107(4):1868–82

Montagner JP, Juhel K, Barsuglia M, Ampuero JP, Chassande-Mottin E, et al. 2016. Prompt gravity signal induced by the 2011 Tohoku-Oki earthquake. *Nat. Commun.* 7:13349

Murray JR, Crowell BW, Grapenthin R, Hodgkinson K, Langbein JO, et al. 2018. Development of a geodetic component for the US West Coast earthquake early warning system. *Seismol. Res. Lett.* 89:2322–36

Nakamura Y. 1988. On the urgent earthquake detection and alarm system (UrEDAS). In *Proceedings of the 9th World Conference on Earthquake Engineering*, Vol. 7, pp. 673–78. Tokyo-Kyoto, Japan: Jpn. Assoc. Earthq. Disaster Prev.

Nakamura Y, Tucker B. 1988. Japan's earthquake early warning system: Should it be imported to California? *Calif. Geol.* 41:33–40

Noda S, Ellsworth WL. 2016. Scaling relation between earthquake magnitude and the departure time from *P* wave similar growth. *Geophys. Res. Lett.* 43(17):9053–60

Noda S, Ellsworth WL. 2017. Determination of earthquake magnitude for early warning from the time dependence of *P*-wave amplitudes. *Bull. Seismol. Soc. Am.* 107(4):1860–67

Noda S, Yamamoto S, Ellsworth WL. 2016. Rapid estimation of earthquake magnitude from the arrival time of the peak high-frequency amplitude. *Bull. Seismol. Soc. Am.* 106(1):232–41

Nof RN, Allen RM. 2016. Implementing the ElarmS earthquake early warning algorithm on the Israeli Seismic Network. *Bull. Seismol. Soc. Am.* 106:2332–44

Ohta Y, Kobayashi T, Tsushima H, Miura S, Hino R, et al. 2012. Quasi real-time fault model estimation for near-field tsunami forecasting based on RTK-GPS analysis: application to the 2011 Tohoku-Oki earthquake ($M_w$ 9.0). *J. Geophys. Res. Solid Earth* 117(B2):B02311

Olson EL, Allen RM. 2005. The deterministic nature of earthquake rupture. *Nature* 438(7065):212–15

Perol T, Gharbi M, Denolle M. 2018. Convolutional neural network for earthquake detection and location. *Sci. Adv.* 4(2):e1700578

Porter K, Shoaf K, Seligson H. 2006. Value of injuries in the Northridge earthquake. *Earthq. Spectra* 22:555–63

Ross ZE, Meier MA, Hauksson E, Heaton TH. 2018. Generalized seismic phase detection with deep learning. *Bull. Seismol. Soc. Am.* 108:2894–901

Ruhl CJ, Melgar D, Chung AI, Grapenthin R, Allen RM. 2019a. Quantifying the value of real-time geodetic constraints on earthquake early warning using a global seismic and geodetic dataset. arXiv:1901.11124 [physics.geo-ph]

Ruhl CJ, Melgar D, Geng J, Goldberg DE, Crowell BW, et al. 2019b. A global database of strong-motion displacement GNSS recordings and an example application to PGD scaling. *Seismol. Res. Lett.* 90(1):271–79

Ruhl CJ, Melgar D, Grapenthin R, Allen RM. 2017. The value of real-time GNSS to earthquake early warning. *Geophys. Res. Lett.* 44(16):8311–19

Rydelek P, Horiuchi S. 2006. Earth science: Is earthquake rupture deterministic? *Nature* 442(7100):E5

Satriano C, Elia L, Martino C, Lancieri M, Zollo A, Iannaccone G. 2010. PRESTo, the earthquake early warning system for southern Italy: concepts, capabilities and future perspectives. *Soil Dyn. Earthq. Eng.* 31:137–53

Saunders JK, Goldberg DE, Haase JS, Bock Y, Offield DG, et al. 2016. Seismogeodesy using GPS and low-cost MEMS accelerometers: perspectives for earthquake early warning and rapid response. *Bull. Seismol. Soc. Am.* 106:2469–89

Seki T, Okada T, Ikeda M, Sugano T. 2008. Early warning "area mail." *NTT Tech. Rev.* 6(12):1–6

Sheen D-H, Park J-H, Chi H-C, Hwang E-H, Lim I-S, et al. 2017. The first stage of an earthquake early warning system in South Korea. *Seismol. Res. Lett.* 88(6):1491–98

Shoaf KI, Nguyen LH, Sareen HR, Bourque LB. 1998. Injuries as a result of California earthquakes in the past decade. *Disasters* 22:218–35

Strauss JA, Allen RM. 2016. Benefits and costs of earthquake early warning, *Seismol. Res. Lett.* 87(3):765–72

Tréhu AM, Wilcock WS, Hilmo R, Bodin P, Connolly J, et al. 2018. The role of the Ocean Observatories Initiative in monitoring the offshore earthquake activity of the Cascadia subduction zone. *Oceanography* 31(1):104–13

Vallée M, Ampuero JP, Juhel K, Bernard P, Montagner JP, Barsuglia M. 2017. Observations and modeling of the elastogravity signals preceding direct seismic waves. *Science* 358(6367):1164–68

Webb SC. 1998. Broadband seismology and noise under the ocean. *Rev. Geophys.* 36(1):105–42

Wood MM, Mileti DS, Kano M, Kelley MM, Regan R, Bourque LB. 2012. Communicating actionable risk for terrorism and other hazards. *Risk Anal.* 32(4):601–15

Worden CB, Wald DJ, Allen TI, Lin K, Garcia D, Cua G. 2010. A revised ground-motion and intensity interpolation scheme for ShakeMap. *Bull. Seismol. Soc. Am.* 100(6):3083–96

Wright TJ, Houlié N, Hildyard M, Iwabuchi T. 2012. Real-time, reliable magnitudes for large earthquakes from 1 Hz GPS precise point positioning: the 2011 Tohoku-Oki (Japan) earthquake. *Geophys. Res. Lett.* 39(12):L12302

Wu Y-M, Hsiao N-C, Chin T-L, Chen D-Y, Chan Y-T, Wang K-S. 2014. Earthquake early warning system in Taiwan. In *Encyclopedia of Earthquake Engineering*, ed. M Beer, IA Kougioumtzoglou, E Patelli, S-K Au. Berlin: Springer. **https://doi.org/10.1007/978-3-642-36197-5_99-1**

Wu Y-M, Mittal H, Huang T-C, Yang BM, Jan J-C, Chen SK. 2018. Performance of a low-cost earthquake early warning system (*P*-alert) and shake map production during the 2018 $M_w$ 6.4 Hualien, Taiwan, earthquake. *Seismol. Res. Lett.* 90(1):19–29

Yin L, Andrews J, Heaton T. 2018. Rapid earthquake discrimination for earthquake early warning: a Bayesian probabilistic approach using three-component single-station waveforms and seismicity forecast. *Bull. Seismol. Soc. Am.* 108:2054–67